Water Research 175 (2020) 115656

Contents lists available at ScienceDirect

Water Research

journal homepage: www.elsevier.com/locate/watres

# Co-metabolism of sulfamethoxazole by a freshwater microalga *Chlorella pyrenoidosa*

Qian Xiong [a, b, c, d], You-Sheng Liu [b, c, **], Li-Xin Hu [b, c], Zhou-Qi Shi [a, b, c, d], Wen-Wen Cai [a, b, c, d], Liang-Ying He [b, c], Guang-Guo Ying [b, c, *]

[a] State Key Laboratory of Organic Geochemistry, Guangzhou Institute of Geochemistry, Chinese Academy of Sciences, Guangzhou, 510640, China
[b] SCNU Environmental Research Institute, Guangdong Provincial Key Laboratory of Chemical Pollution and Environmental Safety & MOE Key Laboratory of Theoretical Chemistry of Environment, South China Normal University, Guangzhou, 510006, China
[c] School of Environment, South China Normal University, University Town, Guangzhou, 510006, China
[d] University of Chinese Academy of Sciences, Beijing, 100049, China

ARTICLE INFO

*Article history:*
Received 28 November 2019
Received in revised form
17 February 2020
Accepted 25 February 2020
Available online 28 February 2020

*Keywords:*
Microalgae
Antibiotic
Sulfamethoxazole
Co-metabolism
Transformation products
Biodegradation

ABSTRACT

Microalgae-mediated biodegradation of antibiotics has recently gained increased attention from international scientific community. However, limited information is available regarding microalgae-mediated biodegradation of SMX in a co-metabolic system. Here we investigated the biodegradation of sulfamethoxazole (SMX) by five algal species (*Pseudokirchneriella subcapitata*, *Scenedesmus quadricauda*, *Scenedesmus obliquus*, *Scenedesmus acuminatus* and *Chlorella pyrenoidosa*), and its transformation pathways by *C. pyrenoidosa* in a sodium acetate (3 mM) co-metabolic system. The results showed that the highest SMX dissipation (14.9%) was detected by *C. pyrenoidosa* after 11 days of cultivation among the five tested algal species in the absence of other carbon sources. The addition of sodium acetate (0–8 mM) significantly enhanced the dissipation efficiency of SMX (0.4 μM) from 6.05% to 99.3% by *C. pyrenoidosa* after 5 days of cultivation, and the dissipation of SMX followed the first-order kinetic model with apparent rate constants (k) ranging from 0.0107 to 0.9811 $d^{-1}$. Based on the results of mass balance analysis, biodegradation by *C. pyrenoidosa* was the main mechanism for the dissipation of SMX in the culture medium. Fifteen phase I and phase II metabolites were identified, and subsequently the transformation pathway was proposed, including oxidation, hydroxylation, formylation and side chain breakdown, as well as pterin-related conjugation. The majority of metabolites of SMX were only observed in the culture medium and varied with cultivation time. The findings of the present study showed effective co-metabolism of a sulfonamide by microalgae, and it may be applied in the aquatic environment remediation and wastewater treatment in the future.



## 1. Introduction

Sulfamethoxazole (SMX) is one of the most widely used drugs for human and veterinary medicine due to its ability to inhibit bacteria and protozoa (Ying et al., 2017; Zhang et al., 2009). Following treatment in animals and human, a considerable proportion of sulfonamides could be excreted with unchanged or metabolized forms through feces and urine due to their poor absorbability and degradability in vivo (Zhang et al., 2015). The extensive application of SMX and the low removal efficiency of SMX in wastewater treatment plants (WWTPs) has resulted in its frequent detection in surface water and groundwater with the concentrations ranging from ng/L to μg/L (Kummerer, 2009; Wang and Wang, 2018). The occurrence of SMX in the aquatic environment could exhibit adverse effects on the growth of microorganisms, aquatic plants and fish, and even affect the structure and function of microbial communities (Boxall et al., 2012; Xiong et al., 2019a). Moreover, there is an increasing evidence showing that the

* Corresponding author. SCNU Environmental Research Institute, Guangdong Provincial Key Laboratory of Chemical Pollution and Environmental Safety & MOE Key Laboratory of Theoretical Chemistry of Environment, South China Normal University, Guangzhou, 510006, China.
** Corresponding author. SCNU Environmental Research Institute, Guangdong Provincial Key Laboratory of Chemical Pollution and Environmental Safety & MOE Key Laboratory of Theoretical Chemistry of Environment, South China Normal University, Guangzhou, 510006, China.
*E-mail addresses:* yousheng.liu@m.scnu.edu.cn (Y.-S. Liu), guangguo.ying@m.scnu.edu.cn (G.-G. Ying).

https://doi.org/10.1016/j.watres.2020.115656
0043-1354/

residual SMX would pose potential risks to human health by inducing the development and spread of antibiotic resistance (He et al., 2016). Therefore, it is of great importance to explore sustainable methods to remove SMX from the aquatic environment.

Previous studies revealed that the removal of sulfonamides by conventional activated sludge treatment in WWTPs is usually incomplete (Chen and Xie, 2018), while biodegradation by pure bacteria isolated from activated sludge can enhance the dissipation of SMX, and some species can even completely mineralize SMX (Wang and Wang, 2018). The main concern related to these approaches is the potential for bacteria to develop antibiotic resistance and transfer antibiotic resistance genes (He et al., 2016). Recently, microalgae-mediated biodegradation has received scientific interests and is proved to be an ecofriendly, effective and safe technology to remove antibiotics (Xiong et al., 2018). It has been verified that mixotrophic microalgae have varied capacities to dissipate antibiotics from wastewater or synthetic wastewater through bioadsorption, bioaccumulation and biodegradation processes (Xiong et al., 2018; Zhou et al., 2014). In a recent study by Xiong et al. (2019b), the removal kinetics of sulfamethazine (SMZ) and SMX by *S. obliquus* was investigated, and the dissipation ratios for SMZ (1 mg/L) and SMX (1 mg/L) were calculated as 15.7% and 29.3%, respectively. After 14 days of cultivation, the removal efficiency of SMX and triclosan by *Nannochloris* sp. was found to be 32% and 72%, respectively (Bai and Acharya, 2016). Our previous study has also found that four freshwater green microalgal species exhibited capacity for simultaneous removal of total nitrogen, total phosphorus, metals and some organic compounds in wastewater (Zhou et al., 2014).

Furthermore, recent studies have demonstrated that augmenting wastewater with organic substrates (e.g., glucose and sodium acetate) or other nutrient substrates (e.g., nitrogen and phosphorus sources) to form a co-metabolic system would be an effective strategy to enhance the biodegradation of persistent organic pollutants (Lu et al., 2019; Xiong et al. 2017b, 2018). The biodegradation of ciprofloxacin by *Chlamydomonas mexicana* was obviously increased from 13% to 56% with the addition of sodium acetate as co-metabolic organic substrate (Xiong et al., 2017b). Additional exogenous carbon (glucose, sodium acetate, or methanol) could also significantly accelerate the biodegradation of some acidic drugs (e.g. diclofenac, ibuprofen and naproxen) by *Pseudoxanthomonas* sp. DIN-3 (Lu et al., 2019). The additional organic substrates not only serve to sustain biomass production, but also act as an electron donor for the co-metabolism of the non-growth substrate (Xiong et al., 2018). To our knowledge, however, the co-metabolism of SMX by microalgae remains unknown so far. Moreover, the transformation mechanism and proposed pathways of SMX involved in the co-metabolic system need to be further studied as it is essential to understand the environmental fate and the risk assessment of SMX in the aquatic environment.

Common freshwater green microalgae, such as *Pseudokirchneriella subcapitata*, *Scenedesmus quadricauda*, *Scenedesmus obliquus*, *Scenedesmus acuminatus* and *Chlorella pyrenoidosa*, have been employed for the removal of various contaminants, considering their potential capability for removing various pollutants and potential use as feedstock for bioenergy production or other high value added products (Xiong et al., 2018; Zhou et al., 2014). The objectives of this study were to test and compare five microalgal species as mentioned above for their capacity to dissipate SMX, and then to investigate degradation of SMX with the selected algal species *C. pyrenoidosa* under various co-metabolic conditions. The influence of sodium acetate as a co-metabolic organic substrate on the dissipation of SMX by *C. pyrenoidosa* was further assessed, and the intermediates of SMX were identified using ultra performance liquid chromatography coupled to quadrupole time-of-flight mass spectrometry (UPLC-QTOF-MS), and the possible transformation pathways of biodegradation were proposed.

## 2. Materials and methods

### 2.1. Chemical agents

Sulfamethoxazole (SMX, purity > 99.5%, Table S1) was purchased from Dr. Ehrenstorfer GmbH (Germany). Acetonitrile and methanol (HPLC grade) were acquired from Merck (Germany). Formic acid (HPLC grade, purity ≥ 98%) was supplied by ANPEL Laboratory Technologies (Shanghai, China). Glucose, sodium acetate and sodium formate were purchased from Sigma-Aldrich. Mineral salts such as $NaNO_3$, $Na_2CO_3$ and $K_2HPO_4 \cdot 3H_2O$ (analytical grade) used for preparation of algal growth medium were obtained from Damao Chemical Reagent Factory (Tianjin, China).

### 2.2. Algae culture

*Pseudokirchneriella subcapitata* FACHB-271, *Scenedesmus quadricauda* FACHB-1468, *Scenedesmus obliquus* FACHB-12, *Scenedesmus acuminatus* FACHB-1221 and *Chlorella pyrenoidosa* FACHB-9 used in the experiment were obtained from the Freshwater Algae Culture Collection of the Institute of Hydrobiology, Chinese Academy of Sciences. The microalgal strains were individually inoculated in 250 mL Erlenmeyer flasks containing 150 mL Blue Green Medium (BG11) amended with 1 mL microalgal suspension ($OD_{680} = 1$) in an illumination incubator for 10 days and under the following conditions: 4000 lx; 25 ± 1 °C; 12:12 h light-dark photoperiod; and humidity 60% (Xiong et al., 2019c). To achieve the desired optical density (OD) for further experiments, the microalgal suspension (cultivated for 10 days) was diluted using sterilized BG11 with a visible spectrophotometer (Yoke Instrument, China).

### 2.3. Batch experiments

#### 2.3.1. Microalgal screening and optimization of initial biomass

A pre-experiment was conducted to screen five microalgal species *(P. subcapitata*, *S. quadricauda*, *S. obliquus*, *S. acuminatus and C. pyrenoidosa)* for their capacity of dissipating SMX. Five microalgal species were respectively cultivated for 11 days in 250 mL capacity Erlenmeyer flasks containing 100 mL sterilized BG11 amended with 1 mL microalgal suspension ($OD_{680} = 1$) and 0.4 μM SMX. Subsequently, the effects of the microalgal initial biomass (different initial biomass with $OD_{680}$ of 0.006, 0.012, 0.018, 0.06 and 0.12) on the dissipation of 0.4 μM SMX were also investigated. Samples were collected on day 0, 2, 4, 7 and 11, respectively.

#### 2.3.2. Effects of organic substrates

Owing to its highest dissipation capacity for SMX in the screening experiment, *C. pyrenoidosa* was selected in further experiments. It was cultivated with an initial $OD_{680}$ of 0.06 to screen the most suitable organic substrate for the co-metabolic biodegradation of SMX. The biodegradation of SMX (0.4 μM) was investigated in 250 mL Erlenmeyer flasks containing 100 mL sterilized BG11 with the addition of glucose (1 mM), sodium acetate (1 mM), or sodium formate (1 mM) for 11 days.

Sodium acetate was selected for further experiments as it produced the highest dissipation of SMX. The dissipation of SMX (0.4 μM) exposed to different sodium acetate concentrations (0, 1, 2, 3, 4 and 8 mM) was investigated in 250 mL Erlenmeyer flasks containing 100 mL sterilized BG11 inoculated with the initial $OD_{680}$ of 0.06. All the flasks were incubated in an illumination incubator for microalgal cultivation. The biodegradation kinetics experiments with the addition of sodium acetate were conducted for 5 d with

sampling on every 0.5 d, and all treatments were carried out in triplicate. To assess the chemical effects on algal growth, the biotic controls were conducted with absence of SMX. Abiotic controls were also included with 0.4 μM SMX, but without algae in the medium, under light and darkness conditions, respectively, to measure the abiotic losses (photolysis and hydrolysis) of the target compound from the culture medium.

### 2.4. Analytical methods

#### 2.4.1. Measurement of cell growth

The dry cell weight (DCW) in each treatment was measured according to our previous study (Peng et al., 2014). A linear correlation between $OD_{680}$ and DCW of *C. pyrenoidosa* (g $L^{-1}$) was obtained as follows:

$$DCW = 0.3781 \times OD_{680} + 0.0021 \left(R^2 = 0.9905\right)$$

The specific growth rate μ was calculated using the following equation:

$$\mu = \frac{lnN_t - lnN_0}{t_t - t_0}$$

where $N_t$ is the DCW at time $t_t$ and $N_0$ is the DCW at the beginning of the test ($t_0 = 0$ d).

#### 2.4.2. Sampling and pretreatment

Exactly 2 mL microalgal suspension was sampled at each sampling time and centrifuged at 15,000 rpm for 5 min to separate microalgal cells, and then 1 mL of the supernatant was filtered with a 0.22-syringe filter (ANPEL Laboratory Technologies, China) for analysis of residual concentrations of SMX in the BG11 medium. Meanwhile, 50 mL microalgal sample was gathered to evaluate the bioadsorption, bioaccumulation, and biodegradation of SMX by *C. pyrenoidosa*. The harvested microalgal cell pellets were re-suspended in distilled water (2 mL) and shaken for 2 min to obtain the SMX absorbed on the cell walls (Xiong et al., 2017a). The sample solution was centrifuged again and the supernatant was recovered for analysis of the concentration of SMX adsorbed onto the cell surface. The rest cell pellets were frozen (−20 °C) over night to breakdown the cell walls, and then re-suspended by adding 2 mL of dichloromethane: methanol (1:2, v/v), followed by sonication for 20 min (40 kHz, 2.2 Kw). The extraction was repeated three times. The supernatant recovered by centrifugation at 15,000 rpm for 5 min was used to determine the concentration of bioaccumulated SMX by *C. pyrenoidosa* biomass.

#### 2.4.3. Instrumental analysis of SMX and its transformation products

The quantification of SMX was achieved by using an Agilent 1260 Infinity LC system equipped with a diode array detector (Agilent Technologies, USA) set at 270 nm and an Agilent Eclipse XDB C18 chromatographic column (150 × 4.6 mm, 5 μm). The mobile phase consisted of 60:40 water (acidified by 0.1% formic acid)/acetonitrile at a flow rate of 1.0 mL $min^{-1}$. The injection volume was 100 μL.

The transformation products for SMX were identified by using an Agilent 1290 Infinity LC system equipped with an Agilent 6545 quadrupole-time-of-flight mass spectrometer (UPLC-QTOF-MS). The injection volume was 3 μL. Separation was accomplished using an Agilent Eclipse Plus C18 column (2.1 × 150 mm, 1.8 μm). A gradient program was used with two mobile phases (A: 0.1% formic acid in water; B: acetonitrile) at a flow rate of 0.3 mL $min^{-1}$. The gradient elution started with 10% B and increased to 20% B within 5 min, and then increased to 25% B at 10 min, followed by a linear gradient to 30% B at 15 min, 40% B at 20 min, and then back to the initial conditions (10% B) for 5 min. The Agilent 6545 system was operated with Dual AJS source in positive and negative electrospray ionization (ESI) mode, using the following operation parameters: capillary voltage, 3500 V ESI-/4000 V ESI+; nebulizer pressure, 40 psi; drying gas flow rate, 9.0 L $min^{-1}$; gas temperature, 325 °C sheath gas flow rate, 11 L $min^{-1}$; sheath gas temperature, 350 °C; skimmer voltage, 65 V; octapole 1 rf, 750 V; fragmentor voltage, 175 V. LC-MS accurate mass spectra were recorded across the range 50–750 *m/z* in both positive and negative ion mode. Samples were first screened using MS1 scan mode at a rate of 2.5 spectra/s and then 4 spectra/s for auto-MS/MS mode with three collision energy values (10, 20 and 40 V) for confirmation. When MS/MS spectra were missing, additional injections in targeted MS/MS mode with selected precursor ions were conducted to obtain fragmentation spectra for some metabolites. The identification of transformation products can refer to Baduel et al. (2019), with details being presented in the Supporting Information (Text S1).

### 2.5. Data analysis

In the present study, all experiments were carried out in triplicate and samples were stored at −20 °C prior to analysis. One-way analysis of variance (ANOVA) with Tukey-Kramer multiple comparison test was conducted to analyze statistical differences among data with Graph Pad Prism 5 software ($p < 0.05$).

The dissipation ($P_b$) of SMX by *C. pyrenoidosa* in culture medium was calculated using a previously reported equation (Xiong et al., 2017a) as follows:

$$P_b = (A_t - A_r - A_d - A_a - A_c)\frac{100}{A_t}$$

where $A_t$ is the initial concentration of SMX added into the medium, $A_r$ is the residual quantity of SMX in the medium, $A_d$ is the amount of SMX adsorbed by microalgal cells, $A_a$ is the amount of SMX dissipated by abiotic processes, and $A_c$ is the amount of SMX accumulated in the microalgal cells.

The SMX biodegradation kinetics of *C. pyrenoidosa* were assessed according to the first order model as follows (Peng et al., 2014):

$$C_t = C_0 \times \exp(-kt)$$

where $C_0$ is the initial concentration of SMX at time zero, $C_t$ is the concentration of SMX at time t, and k is the biodegradation rate constant ($d^{-1}$).

## 3. Results and discussion

### 3.1. Microalgal screening

The dissipation capacity for SMX (0.4 μM) of the five microalgal strains (*P. subcapitata*, *S. quadricauda*, *S. obliquus*, *S. acuminatus* and *C. pyrenoidosa*) is listed in Table S2. Among the five species, *C. pyrenoidosa* showed the highest growth rate and dissipation efficiency for SMX (14.9 ± 0.22%) (Fig. 1a and b). Consequently, *C. pyrenoidosa* was chosen for the subsequent biodegradation experiments in this study. Previous studies have demonstrated that *Chlorella genus* has the potential to dissipate various kinds of xenobiotics (Gao et al., 2011; Song et al., 2019; Xiong et al., 2017a; Zhou et al., 2014). *C. vulgaris* was found to be the most effective strain among six wild species for the biodegradation of 1 mg/L levofloxacin (Xiong et al., 2017a), and *Chlorella* sp. *L38* exhibited the potential for accelerating the dissipation of florfenicol from

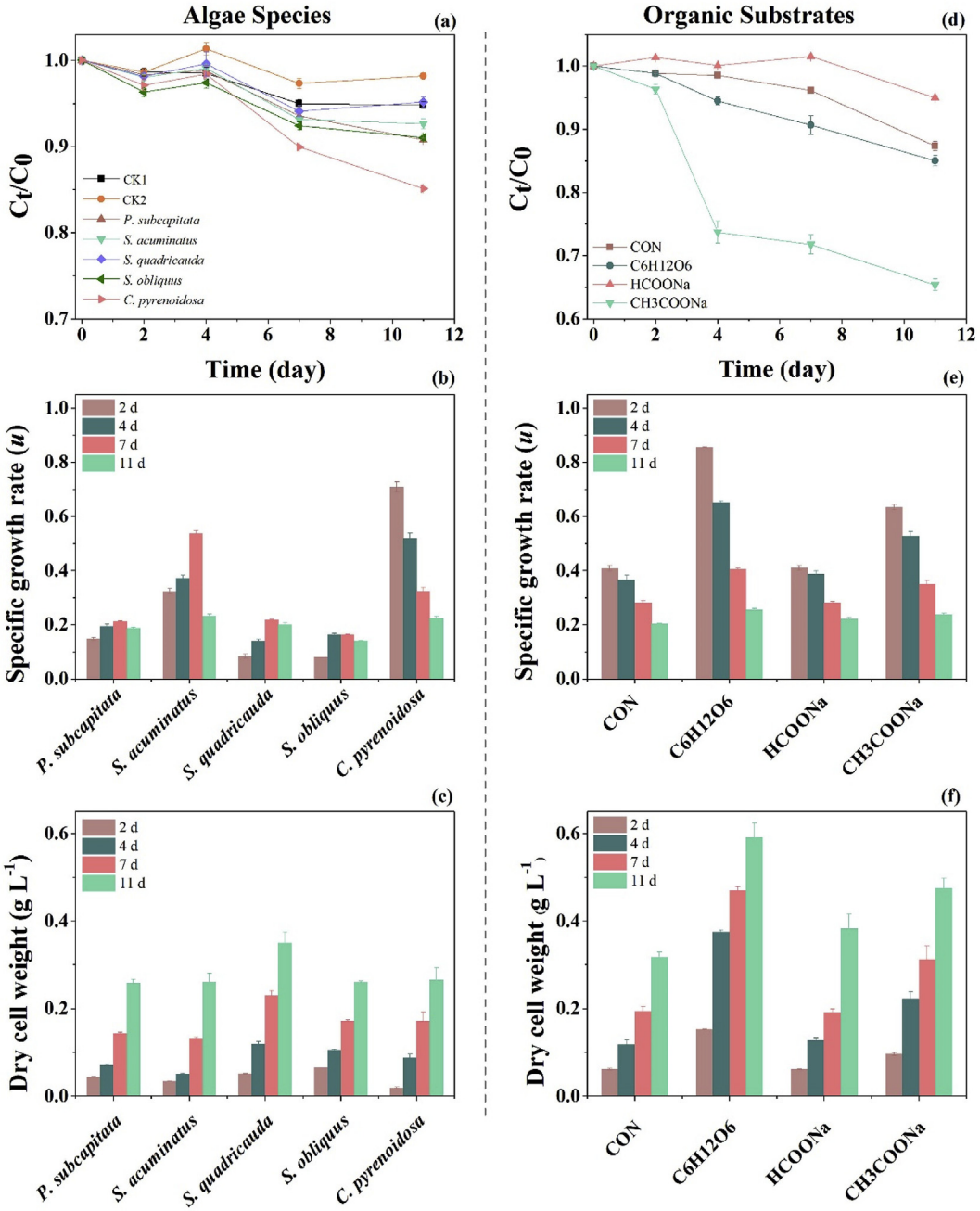


**Fig. 1.** The dissipation capacity of 0.4 μM SMX with different microalgal strains (left) and effects of organic substrates on the dissipation of SMX (right). The dissipation capacity of five microalgal strains (*P. subcapitata*, *S. quadricauda*, *S. obliquus*, *S. acuminatus* and *C. pyrenoidosa*) (a), and difference in the specific growth rate (b) and dry cell weight (c) during 11 days of cultivation. The dissipation kinetics of SMX (d), specific growth rate (e) and dry cell weight (f) of *C. pyrenoidosa* with addition of three different organic substrates (glucose ($C_6H_{12}O_6$) 1 mM, sodium formate (HCOONa) 1 mM and sodium acetate ($CH_3COONa$) 1 mM) during 11 days of cultivation. CK1 and CK2 were two abiotic controls which contained 0.4 μM SMX, but without algae under light and darkness, respectively. CON was blank control which contained 0.4 μM SMX and algae, but without any additional organic substrates. Error bars represent standard deviations (n = 3).

different water sources (Song et al., 2019). It is surprising to find that *S. quadricauda* achieved the highest DCW with 0.35 g $L^{-1}$ after 11 days of cultivation, whilst it showed the lowest SMX dissipation among the five algal strains in the present study (Fig. 1c). These results suggested that cellular composition and structure rather than cell biomass would be responsible for the capability of freshwater algae to biodegrade organic pollutants (Gao et al., 2011). Besides, metabolic and enzymatic activities should be taken into consideration. However, there is a complex enzyme system in microalgae, the exact role of these enzymes in biodegradation requires further investigation (Xiong et al., 2018).

A non-linear relationship between the initial biomass of microalgae and the corresponding dissipation efficiency of contaminants has been found in a previous study (Xiong et al., 2017a). Therefore, the effects of initial biomass on the dissipation efficiency of SMX was investigated in the present study. The dissipation efficiency of SMX by *C. pyrenoidosa* was enhanced with $OD_{680}$ ranged from 0.006 to 0.06, and then decreased with the increasing of $OD_{680}$ until 0.12 (Fig. S1a). Thus, the optimal initial biomass concentration for *C. pyrenoidosa* was selected at $OD_{680}$ = 0.06, as it showed the

highest dissipation efficiency (Fig. S1a). Similar results have been found in the study by Xiong et al. (2017a), where the dissipation efficiency of levofloxacin by *C. vulgaris* decreased with the increasing of initial biomass concentration ($OD_{680}$ = 2.0, 3.0 and 5.0). The DCW of *C. pyrenoidosa* increased with the increase of initial biomass concentration (assessed by $OD_{680}$ values), whereas the specific growth rate of *C. pyrenoidosa* increased until $OD_{680}$ = 0.06 and then decreased with the increase of $OD_{680}$ (Figs. S1b and S1c).

### 3.2. Enhancement effect of sodium acetate as the co-metabolic substrate

The addition of organic substrates or other nutrients has shown the potential for accelerating the biodegradation of antibiotics by microalgae (Xiong et al., 2018). In the present study, three organic substrates (glucose 1 mM, sodium formate 1 mM and sodium acetate 1 mM), which had been proved to be easily biodegradable and thus frequently used as co-substrate (Liang et al., 2019; Xiong et al., 2017b), were applied to evaluate their effects on the dissipation of SMX by *C. pyrenoidosa*. The results indicated that the dissipation of SMX significantly decreased ($p < 0.05$) with the addition of sodium formate (Fig. 1d), which was in accordance to those in a previous study that the dissipation of ciprofloxacin by *Chlamydomonas mexicana* was inhibited with the addition of sodium formate (Xiong et al., 2017b). This negative effect could be related to the catabolite repression, as sodium formate would inhibit the synthesis of enzymes involved in catabolism of carbon sources (Kurade et al., 2011). The dissipation of SMX by *C. pyrenoidosa* was slightly increased from 12.6 to 14.9% in the treatment with glucose as co-metabolic substrate, whilst it significantly increased to 34.6% with sodium acetate as co-metabolic substrate (Fig. 1d).

Moreover, with the presence of sodium formate, glucose and sodium acetate, the DCW of *C. pyrenoidosa* cultivated for 11 days was increased by 20.7%, 85.9% and 49.5%, respectively (Fig. 1e and f), indicating that glucose was the best option for improving the growth of *C. pyrenoidosa*. It was possible that *C. pyrenoidosa* preferred to consume readily degradable carbon source, leading to increased algal growth in the presence of glucose without a corresponding increase in SMX dissipation. Similar results have been observed in a previous study of *Pseudomonas aeruginosa* (Larcher and Yargeau, 2012). The addition of an easily degradable carbon source such as glucose might result in competitive inhibition and consequently weakened the degradation of the target compound (Abtahi et al., 2018). It should be noted that sodium acetate can not only serve as carbon source to sustain algal growth, but also act as an electron donor for co-metabolic degradation of the non-growth substrate (Xiong et al. 2017b, 2018). As a result, sodium acetate was selected as the co-metabolic substrate for the degradation of SMX in the subsequent experiment.

The dissipation of SMX (0.4 μM) was significantly ($p < 0.05$) promoted with addition of sodium acetate comparing to the control group (6.05%). After 5 days of cultivation, the dissipation rate of SMX by *C. pyrenoidosa* achieved to 36.1%, 89.1%, 93.1%, 98.8%, and 99.3% at 1, 2, 3, 4, and 8 mM of sodium acetate, respectively (Fig. 2a). As shown in Table 1, an assumed first order reaction kinetic model was applied to explain the dissipation of SMX (0.4 μM) at different sodium acetate concentrations. Considering the lag phase, the second day of cultivation was set as the initial day of degradation. The apparent dissipation rate constant (k) and the half-lives ($T_{1/2}$) of SMX (0.4 μM) at each concentration of sodium acetate ranged in 0.0107–0.9811 $d^{-1}$ and 0.71–65.08 d, respectively. These results indicated that the dissipation of SMX was increased with the dose of sodium acetate. This was in agreement with the results of a previous study (Liang et al., 2019) that the co-metabolism of some pharmaceuticals such as venlafaxine, tramadol and ciprofloxacin were dependent on the dose of carbon source. In the present study, the dissipation of SMX by *C. pyrenoidosa* was initiated on the second day during the cultivation for all treatments, which may be related to the lag phenomenon in algal growth. In a previous study, an adaptation phase for microorganism was observed with the addition of high concentrations of xenobiotics, leading to a lag phase or change of the kinetics (El-Taliawy et al., 2018). The maximum dissipation rate of SMX occurred on the third day, and subsequently the consumption of SMX by *C. pyrenoidosa* turned to slow down, even reached a plateau on the 4th and 5th day with the treatment of 1 mM sodium acetate. As shown in Fig. 2a and b, a similar trend was found for the dissipation rate of SMX and the growth rate of *C. pyrenoidosa*, implying their potential positive correlation. However, the specific growth rate and DCW of *C. pyrenoidosa* were observed to be inhibited with a high concentration of sodium acetate (4 or 8 mM) (Fig. 2b and c). Liang et al. (2019) found that the influence of acetate on the biodegradation of pharmaceuticals was dose- and compound-dependent, inducing differences in some enzymes involved in the biodegradation. However, further research is still needed to reveal the complex co-metabolism relationship between the dissipation of SMX and dose of sodium acetate.

The mass balance of SMX dissipation by *C. pyrenoidosa* (Table 2) was calculated to reveal the potential enhancing mechanisms of sodium acetate, including biodegradation, bioaccumulation and bioadsorption (Xiong et al., 2018). As shown in Table 2, the dissipation of SMX via abiotic processes was 4.08%. This result was consistent with that found in a previous study, in which insignificant dissipation of SMX by *S. obliquus* was found by abiotic processes (Xiong et al., 2019b). These observations suggested that the dissipation of SMX from medium was mediated by the biotic processes of *C. pyrenoidosa*. Based on the results that bioaccumulation was not observed in any group, biomass uptake and biodegradation were supposed as the main dissipation mechanisms of SMX in the present study. Generally, biomass uptake consisted of an initial rapid and passive adsorption, and subsequently slow, active absorption (Wang et al., 2018). However, surface adsorption caused by *C. pyrenoidosa* was accounted for only a small part in the dissipation of SMX (Table 2). The amount of SMX detected on the surface of *C. pyrenoidosa* was not enough to compensate for the depletion of SMX from culture medium. Meanwhile, majority metabolites of SMX (Fig. 3) were detected in culture medium and varied over time during the 5 days of cultivation. Therefore, it was postulated that biotransformation would be the main process responsible for the loss of SMX in culture medium. Combining our results with those in previous studies (Wang et al., 2018), it can be concluded that SMX was adsorbed by *C. pyrenoidosa*, and then biotransformed into other metabolites, which were subsequently released into medium.

### 3.3. Identified products and proposed transformation pathways

Potential transformation products (TPs) of SMX were identified based on the accurate mass-to-charge ratios ($m/z$) and possible molecular formulas, and their chemical structures were subsequently confirmed by the characteristic fragment ions. The mass spectra information and proposed structures of SMX and its main TPs are summarized in Table S3, while extracted ion chromatograms and the high-resolution mass spectra are shown in Fig. S2 and Fig. S3, respectively. To obtain more information about the actual biotransformation pathways, the area-time trends of SMX and its TPs are presented in Fig. 3. Based on these results, the transformation pathways for SMX are proposed in Fig. 4. The algal transformation of SMX was divided into two major pathways: A) α, β, γ, δ and ε cleavage; and B) reactions of the amine group on the

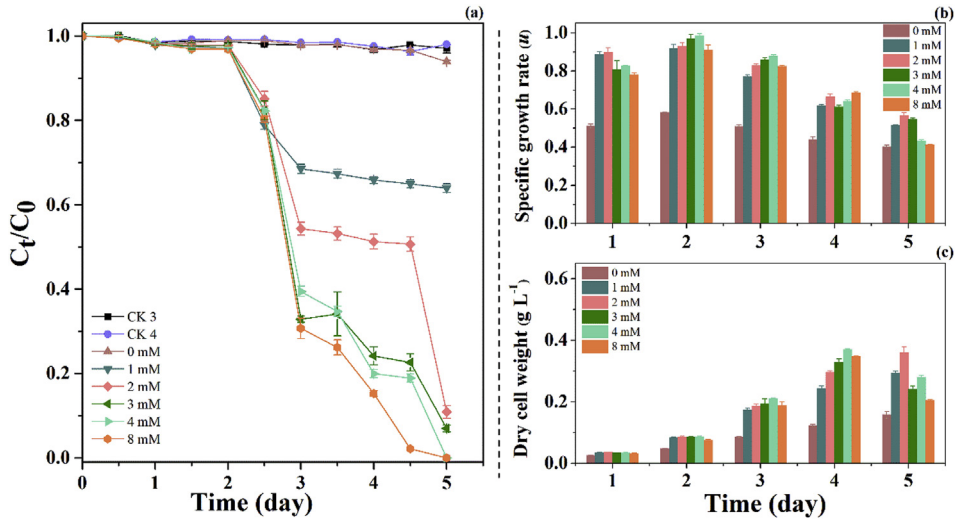


**Fig. 2.** The dissipation kinetics of SMX (0.4 μM) by *C. pyrenoidosa* with the addition of different concentrations of sodium acetate (0, 1, 2, 3, 4 and 8 mM) (a). The changes in the specific growth rate (b) and dry cell weight (c) of *C. pyrenoidosa* during 5 days of cultivation. CK3 and CK4 were two abiotic controls which contained 0.4 μM SMX in the medium, but without algae under light and darkness, respectively. Error bars represent standard deviations (n = 3).

**Table 1**
Kinetic parameters and total dissipation of 0.4 μM SMX by *C. pyrenoidosa* with different sodium acetate concentrations after 5 days of cultivation. Error values represent standard deviations (n = 3).

| Sodium Acetate Concentration (mM) | k [a] ($d^{-1}$) | $T_{1/2}$ [b] (d) | $R^2$ [c] | Total dissipation (%) |
|---|---|---|---|---|
| 0 | 0.0107 ± 0.0005 | 65.1 ± 3.19 | 0.93 | 6.05 ± 0.28 |
| 1 | 0.0349 ± 0.0025 | 19.9 ± 1.50 | 0.99 | 36.1 ± 1.01 |
| 2 | 0.0567 ± 0.0049 | 12.3 ± 1.09 | 0.98 | 89.1 ± 1.48 |
| 3 | 0.2348 ± 0.0051 | 2.95 ± 0.06 | 0.94 | 93.1 ± 2.03 |
| 4 | 0.7188 ± 0.0231 | 0.96 ± 0.03 | 0.95 | 98.8 ± 1.03 |
| 8 | 0.9811 ± 0.0013 | 0.71 ± 0.01 | 0.94 | 99.3 ± 2.71 |

The lag-time was not taken account for the calculation of kinetic parameters based on an assumed first order kinetic reaction.
[a] Kinetic rate constant, calculated using the first-order reaction kinetic model.
[b] Half-life, calculated as (ln 2)/k.
[c] Correlation coefficient, which represents the fitness of the modeling data.

**Table 2**
Mass balance of SMX (0.4 μM) in terms of biodegradation, bioaccumulation, bioadsorption and abiotic processes after 5 days of cultivation.

| Sodium Acetate (mM) | Mass balance of SMX dissipation (%) | | | | |
|---|---|---|---|---|---|
| | Biodegradation | Bioaccumulation | Bioadsorption | Abiotic dissipation | Total dissipation |
| 0 | 0.49 ± 0.03 | ND | 1.48 ± 0.08 | 4.08 ± 0.27 | 6.05 ± 0.28 |
| 1 | 30.3 ± 0.23 | ND | 1.68 ± 0.32 | | 36.1 ± 1.01 |
| 2 | 82.7 ± 0.65 | ND | 2.31 ± 0.37 | | 89.1 ± 1.48 |
| 3 | 84.3 ± 0.54 | ND | 4.73 ± 0.12 | | 93.1 ± 2.03 |
| 4 | 89.6 ± 0.87 | ND | 5.09 ± 0.61 | | 98.8 ± 1.03 |
| 8 | 89.2 ± 0.73 | ND | 6.28 ± 0.72 | | 99.3 ± 2.71 |

ND – Not detected. The SMX concentrations were below the detection limits of HPLC.

benzene ring including oxidation and hydroxylation, as well as pterin-related conjugation.

Under the analytical conditions applied to the UPLC-QTOF-MS, SMX was detected at 7.360 min with the molecular ion $[M+H]^+$ of *m/z* 254.0599 and exhibited characteristic fragmentation patterns of sulfonamide antibiotics. Consistent with a previous study (Huynh and Reinhold, 2019), three common characteristic product ions originating from the 4-aminobenzenesulfonamide moiety (*m/z* 92.0498, 108.0446, and 156.0116) and additional product ions characteristic for SMX (*m/z* 99.0555) were observed with 20 V collision energy. In pathway A, the cleavage of the S–N bond was observed, resulting in the generation of products TP157 (4-aminobenzenesulfinic acid, 4ABSA) and TP98 (3-amino-5-methylisoxazole, 3A5MI). A previous study found that S atom of the sulfonamide group was the most vulnerable site which could be attacked to break down the functional groups (Yin et al., 2017). Similar TPs were identified in the biodegradation of SMX by *S. obliquus* as reported in a previous study (Xiong et al., 2019b). 3A5MI was one of the most frequently detected TPs in SMX biodegradation (Chen and Xie, 2018). It was suggested that TP157 would further undergo a reaction from the loss of $SO_2$ group (TP93), followed by addition of hydroxyl group on the benzene ring and then oxidation (TP107). A similar pathway was proposed in the catalytic oxidation of SMX by peroxymonosulfate activation (Bao et al., 2019). A previous study indicated that formylation was one of the main biotransformation reactions of SMX (Majewsky et al., 2015).

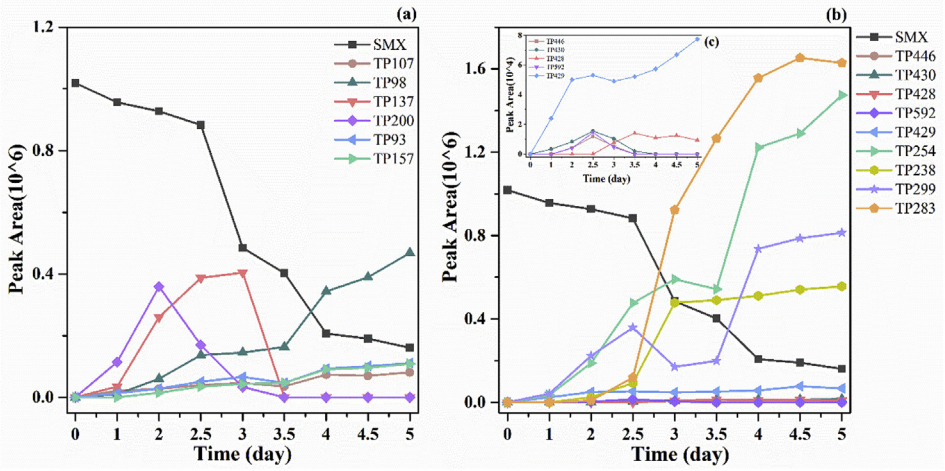


**Fig. 3.** Changes in the abundance of SMX and its transformation products with the reaction time by *C. pyrenoidosa* in a co-metabolic system with sodium acetate. (a), transformation products from pathway A; (b), transformation products from pathway B; (c), enlarged graph of five pterin-related transformation products.

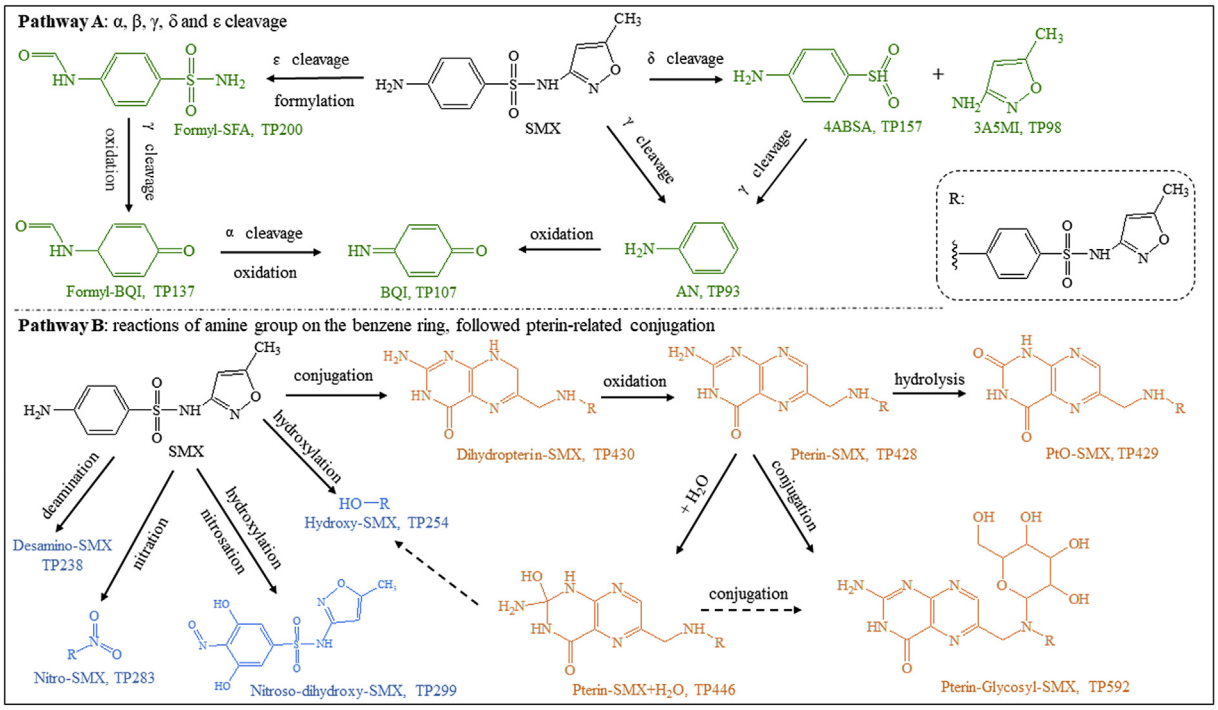


**Fig. 4.** Proposed transformation pathways of SMX by *C. pyrenoidosa* in a co-metabolic system with sodium acetate. TPs colored with green generated from α, β, γ, δ and ε cleavage; orange, from the conjugation with pterin; blue, from oxidation of the amine group on the benzene ring. The structures in brackets represent suggested intermediates. (For interpretation of the references to color in this figure legend, the reader is referred to the Web version of this article.)

Although formyl-SMX was not observed in the present study, two related TPs (TP200 and TP137) were found. With the cleavage of N–C bond, sulfanilamide would originate, followed by the formylation of amine group to generate TP200. And TP137 might generate from TP200 with the cleavage of C–S bond and subsequent oxidation. As shown in Fig. 3a, the abundance of TP107, TP98, TP93 and TP157 showed an increasing trend with the extending of cultivation time. The abundance of TP200 increased rapidly in the first 2 days and then decreased, whilst TP137 reached a top level on the third day, implying the formation of TP137 from TP200.

In pathway B, TPs marked in blue were mainly from the reaction of amine group on the benzene ring (Fig. 4). The N atom on the benzene ring was the most susceptible sites to be attacked to form nitroso- or nitro-group adducted SMX (Yin et al., 2018). Nitro-SMX (TP283) was detected in the present study, and an increasing trend for its abundance was observed with extension of cultivation time (Fig. 3b). However, nitroso-SMX was absent in the present study, implying further reactions might have occurred, as nitroso-SMX might be further oxidized to generate TP299 (Nitroso-dihydroxy-SMX) via the substitution of hydrogen with hydroxyl group on the benzene ring. TP254 (Hydroxy-SMX) could be generated from SMX by the substitution of amine group with hydroxyl group and subsequently into TP238 (Desamino-SMX) via dehydroxylation. SMX could also be transformed into TP238 via deamination, which has been found in the biodegradation of SMX by ammonia oxidizing bacteria (Kassotaki et al., 2016). Previous studies have

demonstrated that nitration, nitrosation, hydroxylation and deamination of the amine group on the benzene ring were the main biotransformation reactions for sulfonamides (Deng et al., 2016; Majewsky et al., 2015), which was in line with the results in the present study. As presented in Fig. 3b, the four TPs generated from the reactions of amine group on the benzene ring showed increasing trends from day 2 to the final sampling point.

Moreover, five conjugated TPs (marked in orange) were identified in pathway B (Fig. 4). TP429 (*m/z* 430.0923, RT 7.226 min) was initially thought to be a glucuronide conjugation product, while its $MS^2$ spectrum could not correspond with the glucuronide conjugation found in *Arabidopsis thaliana* cell (Dudley et al., 2018). A second TP with *m/z* 429.1086 (TP428, RT 6.539 min) exhibited fragments at *m/z* 176.0651, 267.0982, 283.0930, 331.0594 and 349.0723 under the collision energy of 20 V (Fig. S2), which have been previously identified as characteristic fragments of a Pterin-SMX conjugate (Richter et al., 2013; Stravs et al., 2017). The TP429 (PtO-SMX) could then be explained as a product of Pterin-SMX, where the primary amine has been transformed to a keto group. The formation of pterin-sulfonamide conjugates has been found in the biotransformation of sulfonamides with bacteria (Richter et al., 2013) and microalgae (Stravs et al., 2017), and even in activate sludge (Achermann et al., 2018), which was relevant to the mode of action of sulfonamides. Sulfonamides act as inhibitors of dihydropteroate synthase (DHPS), which catalyzes the formation of dihydropteroate from dihydropterin pyrophosphate and *p*-aminobenzoic acid (*p*ABA). In addition to inhibiting DHPS, sulfonamides can also act as an alternative enzyme substrate promoting the formation pterin-sulfonamide conjugates (Richter et al., 2013; Zhao et al., 2016). Another related product TP430 (Dihydropterin-SMX, *m/z* 431.1235) was observed at 6.332 min, which was the dihydro form of pterin-SMX. Theoretically, dihydropterin-sulfonamides were originated during the enzymatic reaction between sulfonamides and DHPS (Zhao et al., 2016). In accordance with the studies of Richter et al. (2013) and Stravs et al. (2017), Dihydropterin-SMX appeared prior to Pterin-SMX and PtO-SMX but disappeared before the final sampling point (Fig. 3c). With spiking of pterin-sulfathiazole into activated sludge, Achermann et al. (2018) further demonstrated the pathway of pterin-related biotransformation. From the present study and previous studies, it revealed that Pterin-SMX was the stable form of Dihydropterin-SMX, and it could lead to further formation of PtO-SMX.

Meanwhile, another one pterin-related conjugation TP, Hydroxy-Pterin-SMX (TP446, *m/z* 447.1210, RT 3.262 min), was observed. Additionally, TP592 eluted at a retention time of 7.004 with the accurate mass of *m/z* 591.1651, with loss of one anhydroglucoe moiety during 20 V collision energy fragmentation, revealing Pterin-SMX and its five signature fragments. Consequently, TP592 was determined to be a pterin glycosyl conjugate of SMX, which likely formed from Pterin-SMX (TP428). Glycosylated metabolites have been commonly observed in plants, as a detoxifying mechanism for xenobiotic-exposed (Huynh and Reinhold, 2019). TPs formed from glycosylate conjugation were also detected in the biotransformation of triclosan by three different microalgal species (Wang et al., 2018). Unlike the other three pterin-related TPs, the abundance of TP446 and TP592 spiked on day 2.5 and subsequently disappeared as shown in Fig. 3c.

As shown in Fig. 4, biodegradation of SMX might undergo phase I reactions including oxidation and hydroxylation reactions of the amine group, which was followed by phase II reactions through formylation and conjugation. The metabolites generated from phase I reactions would increase the polarity and hydrophilicity of the xenobiotics and thus facilitate the excretion of the toxic compounds. Moreover, products of phase I might conjugate with large and polar compounds (e.g. sugars and amino acids) in phase II reactions to further increase the water solubility of xenobiotics (Dudley et al., 2018; Torres et al., 2008). The formation of transformation products might be catalyzed by the species-specific enzyme systems of algae for detoxification in response to the toxic pollutants (Wang et al., 2018). The detoxification metabolisms carried out by cytochrome P450 (CYP450) might be responsible for the biotransformation of xenobiotics (Torres et al., 2008). Some products were reported for the first time in the present study, indicating different transformation mechanisms of SMX by *C. pyrenoidosa* in a co-metabolic system, though majority products detected in the present study have been frequently reported in previous studies. Compared to the study of Xiong et al. (2019b), more TPs were found in our study, especially those from phase II reactions. The addition of sodium acetate might have effects on the parent compounds, transformation products and transformation pathways (Liang et al., 2019).

Metabolism of SMX by microalgae (Stravs et al., 2017; Xiong et al., 2019b) and plants (Chen et al., 2017; Dudley et al., 2018; Huynh and Reinhold, 2019) has been reported in recent studies. Although accumulation of SMX was universal, results as to its metabolic fate in biota drastically differ (Huynh and Reinhold, 2019). For instance, several metabolites of SMX were observed in *A. thaliana* cells (Dudley et al., 2018), while no metabolites were detected in Chinese cabbage and water spinach exposed to 100 μg/mL SMX (Chen et al., 2017). In the present study, accumulation of SMX was not observed in algal cells, and contributions from bioadsorption and abiotic processes accounted for a small part of SMX loss, thus biotransformation would be the main mechanism for the dissipation of SMX in culture medium. Subsequently, TPs from phase I and II reactions were observed in culture medium and varied with cultivation time, which might be attributed to algal excretion. Similarly, it was demonstrated that triclosan was adsorbed by algal cells, then biotransformed into some metabolites, and subsequently released into the medium (Wang et al., 2018). Based on these findings, a growing body of evidence indicates that algal excretion of metabolites may be an additional defense mechanism against the toxicity of xenobiotics (Khan et al., 2016).

## 4. Conclusions

In this study, *C. pyrenoidosa* showed the highest capacity of SMX dissipation among five green freshwater microalgae species. The dissipation of SMX was significantly enhanced with the addition of sodium acetate as co-metabolic substrate. It is concluded that biotransformation was the predominant mechanism for the depletion of SMX by *C. pyrenoidosa*. The co-metabolic pathway of SMX by *C. pyrenoidosa* was firstly proposed, involving the breakdown of side chain, reactions of the amine group on the benzene ring (oxidation and hydroxylation), and pterin-related conjugation. Although no obviously adverse effects were observed on the growth of *C. pyrenoidosa*, the formation of pterin-SMX conjugation might potentially impair folate biosynthesis. Thus, future studies are needed to investigate the fate and toxicity of transformation products of SMX.

## Notes

The authors declare no competing financial interest.

## Declaration of competing interest

The authors declare that they have no known competing financial interests or personal relationships that could have appeared to influence the work reported in this paper.

## Acknowledgements

The authors would like to acknowledge the financial support from the National Natural Science Foundation of China (NSFC U1701242 and 41877359).

## Appendix A. Supplementary data

Supplementary data to this article can be found online at https://doi.org/10.1016/j.watres.2020.115656.

## References

Abtahi, S.M., Petermann, M., Juppeau Flambard, A., Beaufort, S., Terrisse, F., Trotouin, T., Joannis Cassan, C., Albasi, C., 2018. Micropollutants removal in tertiary moving bed biofilm reactors (MBBRs): contribution of the biofilm and suspended biomass. Sci. Total Environ. 643, 1464–1480.

Achermann, S., Bianco, V., Mansfeldt, C.B., Vogler, B., Kolvenbach, B.A., Corvini, P.F.X., Fenner, K., 2018. Biotransformation of sulfonamide antibiotics in activated aludge: the formation of pterin-conjugates leads to sustained risk. Environ. Sci. Technol. 52 (11), 6265–6274.

Baduel, C., Lai, F.Y., van Nuijs, A.L.N., Covaci, A., 2019. Suspect and nontargeted strategies to investigate in vitro human biotransformation products of emerging environmental contaminants: the benzotriazoles. Environ. Sci. Technol. 53 (17), 10462–10469.

Bai, X.L., Acharya, K., 2016. Removal of trimethoprim, sulfamethoxazole, and triclosan by the green alga *Nannochloris* sp. J. Hazard Mater. 315, 70–75.

Bao, Y., Oh, W.D., Lim, T.T., Wang, R., Webster, R.D., Hu, X., 2019. Elucidation of stoichiometric efficiency, radical generation and transformation pathway during catalytic oxidation of sulfamethoxazole via peroxymonosulfate activation. Water Res. 151, 64–74.

Boxall, A.B.A., Rudd, M.A., Brooks, B.W., Caldwell, D.J., Choi, K., Hickmann, S., Innes, E., Ostapyk, K., Staveley, J.P., Verslycke, T., Ankley, G.T., Beazley, K.F., Belanger, S.E., Berninger, J.P., Carriquiriborde, P., Coors, A., DeLeo, P.C., Dyer, S.D., Ericson, J.F., Gagné, F., Giesy, J.P., Gouin, T., Hallstrom, L., Karlsson, M.V., Larsson, D.G.J., Lazorchak, J.M., Mastrocco, F., McLaughlin, A., McMaster, M.E., Meyerhoff, R.D., Moore, R., Parrott, J.L., Snape, J.R., Murray-Smith, R., Servos, M.R., Sibley, P.K., Straub, J.O., Szabo, N.D., Topp, E., Tetreault, G.R., Trudeau, V.L., Van Der Kraak, G., 2012. Pharmaceuticals and personal care products in the environment: what are the big questions? Environ. Health Perspect. 120 (9), 1221–1229.

Chen, H.R., Rairat, T., Loh, S.H., Wu, Y.C., Vickroy, T.W., Chou, C.C., 2017. Assessment of veterinary drugs in plants using pharmacokinetic approaches: the absorption, distribution and elimination of tetracycline and sulfamethoxazole in ephemeral vegetables. PloS One 12 (8).

Chen, J., Xie, S., 2018. Overview of sulfonamide biodegradation and the relevant pathways and microorganisms. Sci. Total Environ. 640–641, 1465–1477.

Deng, Y., Mao, Y., Li, B., Yang, C., Zhang, T., 2016. Aerobic degradation of sulfadiazine by *Arthrobacter* spp.: kinetics, pathways, and genomic characterization. Environ. Sci. Technol. 50 (17), 9566–9575.

Dudley, S., Sun, C., Jiang, J., Gan, J., 2018. Metabolism of sulfamethoxazole in *Arabidopsis thaliana* cells and cucumber seedlings. Environ. Pollut. 242 (Pt B), 1748–1757.

El-Taliawy, H., Casas, M.E., Bester, K., 2018. Removal of ozonation products of pharmaceuticals in laboratory moving bed biofilm reactors (MBBRs). J. Hazard Mater. 347, 288–298.

Gao, Q.T., Wong, Y.S., Tam, N.F., 2011. Removal and biodegradation of nonylphenol by different *Chlorella* species. Mar. Pollut. Bull. 63 (5–12), 445–451.

He, L.Y., Ying, G.G., Liu, Y.S., Su, H.C., Chen, J., Liu, S.S., Zhao, J.L., 2016. Discharge of swine wastes risks water quality and food safety: antibiotics and antibiotic resistance genes from swine sources to the receiving environments. Environ. Int. 92–93, 210–219.

Huynh, K., Reinhold, D., 2019. Metabolism of sulfamethoxazole by the model plant *Arabidopsis thaliana*. Environ. Sci. Technol. 53 (9), 4901–4911.

Kassotaki, E., Buttiglieri, G., Ferrando-Climent, L., Rodriguez-Roda, I., Pijuan, M., 2016. Enhanced sulfamethoxazole degradation through ammonia oxidizing bacteria co-metabolism and fate of transformation products. Water Res. 94, 111–119.

Khan, B.R., Wherritt, D.J., Huhman, D., Sumner, L.W., Chapman, K.D., Blancaflor, E.B., 2016. Malonylation of Glucosylated N-Lauroylethanolamine: a new pathway that determines N-acyletjanolamine metabolic fate in plants. J. Biol. Chem. 291 (53), 27112–27121.

Kummerer, K., 2009. Antibiotics in the aquatic environment - a review - Part I. Chemosphere 75 (4), 417–434.

Kurade, M.B., Waghmode, T.R., Govindwar, S.P., 2011. Preferential biodegradation of structurally dissimilar dyes from a mixture by *Brevibacillus laterosporus*. J. Hazard Mater. 192 (3), 1746–1755.

Larcher, S., Yargeau, V., 2012. Biodegradation of sulfamethoxazole: current knowledge and perspectives. Appl. Microbiol. Biotechnol. 96 (2), 309–318.

Liang, C., Zhang, L., Nord, N.B., Carvalho, P.N., Bester, K., 2019. Dose-dependent effects of acetate on the biodegradation of pharmaceuticals in moving bed biofilm reactors. Water Res. 159, 302–312.

Lu, Z., Sun, W., Li, C., Ao, X., Yang, C., Li, S., 2019. Bioremoval of non-steroidal anti-inflammatory drugs by *Pseudoxanthomonas* sp. DIN-3 isolated from biological activated carbon process. Water Res. 161, 459–472.

Majewsky, M., Glauner, T., Horn, H., 2015. Systematic suspect screening and identification of sulfonamide antibiotic transformation products in the aquatic environment. Anal. Bioanal. Chem. 407 (19), 5707–5717.

Peng, F.Q., Ying, G.G., Yang, B., Liu, S., Lai, H.J., Liu, Y.S., Chen, Z.F., Zhou, G.J., 2014. Biotransformation of progesterone and norgestrel by two freshwater microalgae (*Scenedesmus obliquus* and *Chlorella pyrenoidosa*): transformation kinetics and products identification. Chemosphere 95, 581–588.

Richter, M.K., Focks, A., Siegfried, B., Rentsch, D., Krauss, M., Schwarzenbach, R.P., Hollender, J., 2013. Identification and dynamic modeling of biomarkers for bacterial uptake and effect of sulfonamide antimicrobials. Environ. Pollut. 172, 208–215.

Song, C., Wei, Y., Qiu, Y., Qi, Y., Li, Y., Kitamura, Y., 2019. Biodegradability and mechanism of florfenicol via *Chlorella* sp. UTEX1602 and L38: experimental study. Bioresour. Technol. 272, 529–534.

Stravs, M.A., Pomati, F., Hollender, J., 2017. Exploring micropollutant biotransformation in three freshwater phytoplankton species. Environ. Sci. Process. Impacts 19 (6), 822–832.

Torres, M.A., Barros, M.P., Campos, S.C., Pinto, E., Rajamani, S., Sayre, R.T., Colepicolo, P., 2008. Biochemical biomarkers in algae and marine pollution: a review. Ecotoxicol. Environ. Saf. 71 (1), 1–15.

Wang, J., Wang, S., 2018. Microbial degradation of sulfamethoxazole in the environment. Appl. Microbiol. Biotechnol. 102 (8), 3573–3582.

Wang, S., Poon, K., Cai, Z., 2018. Removal and metabolism of triclosan by three different microalgal species in aquatic environment. J. Hazard Mater. 342, 643–650.

Xiong, J.Q., Govindwar, S., Kurade, M.B., Paeng, K.J., Roh, H.S., Khan, M.A., Jeon, B.H., 2019a. Toxicity of sulfamethazine and sulfamethoxazole and their removal by a green microalga, *Scenedesmus obliquus*. Chemosphere 218, 551–558.

Xiong, J.Q., Kim, S.J., Kurade, M.B., Govindwar, S., Abou-Shanab, R.A.I., Kim, J.R., Roh, H.S., Khan, M.A., Jeon, B.H., 2019b. Combined effects of sulfamethazine and sulfamethoxazole on a freshwater microalga, *Scenedesmus obliquus*: toxicity, biodegradation, and metabolic fate. J. Hazard Mater. 370, 138–146.

Xiong, J.Q., Kurade, M.B., Jeon, B.H., 2017a. Biodegradation of levofloxacin by an acclimated freshwater microalga, *Chlorella vulgaris*. Chem. Eng. J. 313, 1251–1257.

Xiong, J.Q., Kurade, M.B., Jeon, B.H., 2018. Can microalgae remove pharmaceutical contaminants from water? Trends Biotechnol. 36 (1), 30–44.

Xiong, J.Q., Kurade, M.B., Kim, J.R., Roh, H.S., Jeon, B.H., 2017b. Ciprofloxacin toxicity and its co-metabolic removal by a freshwater microalga *Chlamydomonas mexicana*. J. Hazard Mater. 323 (Pt A), 212–219.

Xiong, Q., Hu, L.X., Liu, Y.S., Wang, T.T., Ying, G.G., 2019c. New insight into the toxic effects of chloramphenicol and roxithromycin to algae using FTIR spectroscopy. Aquat. Toxicol. 207, 197–207.

Yin, R.L., Guo, W.Q., Du, J.S., Zhou, X.J., Zheng, H.S., Wu, Q.L., Chang, J.S., Ren, N.Q., 2017. Heteroatoms doped graphene for catalytic ozonation of sulfamethoxazole by metal-free catalysis: performances and mechanisms. Chem. Eng. J. 317, 632–639.

Yin, R.L., Guo, W.Q., Wang, H.Z., Du, J.S., Zhou, X.J., Wu, Q.L., Zheng, H.S., Chang, J.S., Ren, N.Q., 2018. Selective degradation of sulfonamide antibiotics by peroxymonosulfate alone: direct oxidation and nonradical mechanisms. Chem. Eng. J. 334, 2539–2546.

Ying, G.G., He, L.Y., Ying, A.J., Zhang, Q.Q., Liu, Y.S., Zhao, J.L., 2017. China must reduce its antibiotic use. Environ. Sci. Technol. 51 (3), 1072–1073.

Zhang, Q.Q., Ying, G.G., Pan, C.G., Liu, Y.S., Zhao, J.L., 2015. Comprehensive evaluation of antibiotics emission and fate in the river basins of China: source analysis, multimedia modeling, and linkage to bacterial resistance. Environ. Sci. Technol. 49 (11), 6772–6782.

Zhang, Y., Marrs, C.F., Simon, C., Xi, C., 2009. Wastewater treatment contributes to selective increase of antibiotic resistance among *Acinetobacter* spp. Sci. Total Environ. 407 (12), 3702–3706.

Zhao, Y., Shadrick, W.R., Wallace, M.J., Wu, Y., Griffith, E.C., Qi, J., Yun, M.K., White, S.W., Lee, R.E., 2016. Pterin-sulfa conjugates as dihydropteroate synthase inhibitors and antibacterial agents. Bioorg. Med. Chem. Lett 26 (16), 3950–3954.

Zhou, G.J., Ying, G.G., Liu, S., Zhou, L.J., Chen, Z.F., Peng, F.Q., 2014. Simultaneous removal of inorganic and organic compounds in wastewater by freshwater green microalgae. Environ. Sci. Process. Impacts 16 (8), 2018–2027.